

## College of Engineering



Drexel E-Repository and Archive (iDEA)

<http://idea.library.drexel.edu/>

Drexel University Libraries

[www.library.drexel.edu](http://www.library.drexel.edu)

The following item is made available as a courtesy to scholars by the author(s) and Drexel University Library and may contain materials and content, including computer code and tags, artwork, text, graphics, images, and illustrations (Material) which may be protected by copyright law. Unless otherwise noted, the Material is made available for non profit and educational purposes, such as research, teaching and private study. For these limited purposes, you may reproduce (print, download or make copies) the Material without prior permission. All copies must include any copyright notice originally included with the Material. **You must seek permission from the authors or copyright owners for all uses that are not allowed by fair use and other provisions of the U.S. Copyright Law.** The responsibility for making an independent legal assessment and securing any necessary permission rests with persons desiring to reproduce or use the Material.

Please direct questions to [archives@drexel.edu](mailto:archives@drexel.edu)

# **Application of zonal model on indoor air sensor network design**

Y. Lisa Chen and Jin Wen

Civil, Architectural, and Environmental Engineering Department,  
Drexel University, Philadelphia, PA, 19104

## **ABSTRACT**

Growing concerns over the safety of the indoor environment have made the use of sensors ubiquitous. Sensors that detect chemical and biological warfare agents can offer early warning of dangerous contaminants. However, current sensor system design is more informed by intuition and experience rather than systematic design. To develop a sensor system design methodology, a proper indoor airflow modeling approach is needed. Various indoor airflow modeling techniques, from complicated computational fluid dynamics approaches to simplified multi-zone approaches, exist in the literature. In this study, the effects of two airflow modeling techniques, multi-zone modeling technique and zonal modeling technique, on indoor air protection sensor system design are discussed. Common building attack scenarios, using a typical CBW agent, are simulated. Both multi-zone and zonal models are used to predict airflows and contaminant dispersion. Genetic Algorithm is then applied to optimize the sensor location and quantity. Differences in the sensor system design resulting from the two airflow models are discussed for a typical office environment and a large hall environment.

Keywords: indoor air quality, multi-zone modeling, zonal modeling, chemical and biological warfare (CBW) agent, sensor system design

## 1. INTRODUCTION

Sensors are currently used in the building environment to monitor temperature and humidity. Parameters such as contaminant levels are also of importance when evaluating indoor air quality. Recently, the public and those involved in heating, ventilating, and air conditioning (HVAC) design have begun to focus on safety issues in the building environment. Specifically, by the potential for terrorist attacks by means of the release of chemical and biological warfare (CBW) agents inside buildings. Since HVAC systems circulate air throughout buildings, they can also serve to spread released CBW agents very rapidly around buildings. Properly placed sensors can help to reduce the deleterious effects of such attacks by alerting building occupants early. The current method in sensor system design is based on past design experience. The number of sensors to install and where to install them are decided by intuition rather than by formal practices. Sensors used to measure indoor pollutants including CBW agents have complicated characteristics, which presents an opportunity to combine sensors with different characteristics to form an optimal sensor system.

To design sensor systems for indoor air environment, indoor airflow and contaminant dispersion patterns need to be known. Several airflow modeling approaches, namely, computational fluid dynamics (CFD), multi-zone modeling, and zonal modeling, exist in the literature. First, CFD is the numerical solution of the governing equations of fluid motion and contaminant dispersion. For decades, numerous studies have validated CFD results.

Nevertheless, running a CFD simulation requires the user to have specific knowledge on fluid mechanics and on numerical techniques. It is also computationally intense.

Second, multi-zone models represent any building as a network of well-mixed zones. In other words, temperature, humidity, mass flow and contaminant concentration do not vary with respect to space within each zone. Furthermore, zones are connected by discrete flow paths, such as doors, windows, and cracks. Though computationally efficient compared to CFD models, multi-zone models cannot provide detailed airflow (or contaminant dispersion) within a zone. However, a recent release of CONTAM (version 2.4) includes a "One-Dimensional Convection/Diffusion" model that is able to consider concentration gradients along a specified axis in a zone and through a ducted HVAC system [1].

Lastly, zonal models sub-divide larger zones into sub-zones in order to offer a more realistic representation of airflows and contaminant concentration within zones. Many classes of zonal models have been reported in the literature and are summarized by Mora et al. [2]. The approaches are: power-law (PL), power-law with specific driven flow (PL-SDF), surface drag (SD), and surface drag with specific driven flow (SD-SDF). SD modeling eliminates the dependence of the simulated pressure drop on the number of cells used, which PL models exhibit. SDF modeling addresses the representation of jets and plumes. The study compared the results of each zonal model with CFD models with regards to air flow patterns, velocity profiles, and pressure predictions. The resulting air flow patterns for the PL and SD models were similar, as were the PL-SDF and SD-SDF models. Both the PL and SD models resulted in unidirectional (no recirculation) air flows and no wall jet from the diffuser. Both the PL-SDF and SD-SDF models predicted the wall jet. However, still no recirculation inside the room air is predicted. On the other hand, CFD models of varying grid sizes clearly show the wall jet, recirculation, and entrainment of the room air into the inlet jet. Thus, as expected, the CFD model was able to model airflow much more accurately than the zonal models. However, it remains to be seen whether the improved accuracy provided by the CFD model is necessarily appropriate for sensor system design.

Several studies ([3] to [4]) exist in the literature that discuss sensor system design systematically and are summarized by Chen and Wen [3]. CFD models were used by Zhai et al. [5] and Arvelo et al [4] to simulate airflow and contaminant dispersion. Chen and Wen [3] studied the use of a multi-zone airflow model for CBW sensor design. However, the effects of different airflow modeling approaches on indoor pollutant sensor system design have not been reported in the literature. Thus, the objective of this study is to examine the impact of different airflow modeling approaches on sensor system design. This is done by comparing the sensor system design results using both a multi-zone airflow model, COMIS3.0 [6] and a zonal airflow model, COwZ [7].

## 2. SIMULATION MODEL

The airflow pattern and contaminant dispersion after the release of a CBW agent is modeled in this study using both a multi-zone airflow model, COMIS3.0 and COwZ. Genetic Algorithm (GA) is the optimization approach chosen for sensor system design. Validation of zonal models in the literature is first discussed in Sec. 2.1. COwZ is then introduced in Sec. 2.2. Sections 2.3 and 2.4 then introduce the two spaces that are modeled in this study and the releasing scenarios, respectively. A detailed discussion on GA can be found in [3].

## 2.1 Zonal Models

Several studies in the literature have validated results from zonal models with both CFD and experimental data. The discussion here is not exhaustive but serves to demonstrate the principles of zonal models. Comparisons of airflows from several zonal models with CFD results were presented by Mora et al. [2]. Musy et al. [8] used a zonal model to predict temperature gradients created by an electric heater in a small room. Results for temperature agreed well with experimental data. Inard et al. [9] used a zonal model to predict airflows in various flow conditions including natural convection and mixed convection. Again, the model produced satisfactory results when compared with experimental data. Wurtz et al. [10] examined results from zonal models, CFD models, and experimental data. The study concluded that temperature differences are small while airflow differences are largest near wall surfaces. Haghghat et al. [11] compared results from two zonal models, theirs and other researchers, CFD models, and experimental data. It was shown that the zonal model was able to predict recirculation patterns observed experimentally and predicted by CFD.

## 2.2 COWZ

A zonal model, COWZ, which is sub-zones nested within the multi-zone model, COMIS3.0 [6] is used in this study. COWZ was developed to simulate building airflow and contaminant dispersion. According to the discussion on the various classes of zonal models, COWZ can be classified as the PL-SDF type.

In COWZ, sub-zones are designated as either "standard" sub-zones or "mixed" sub-zones. Flow between standard sub-zones is primarily driven by pressure forces. A power-law relation, used for modeling large openings, is applied to flow between standard sub-zones. The mass flow between two standard sub-zones is [12]:

$$m_{j,i} = C_d \rho (\Delta p_{j,i})^n A \quad (1)$$

where  $A$  is the area ( $\text{m}^2$ ) of the interface between sub-zones  $i$  and  $j$ ,  $C_d$  is the discharge coefficient ( $0.83 \text{ m s}^{-1} \text{ Pa}^{-n}$  is commonly used [10]),  $n$  is the power-law exponent (taken to be 0.5),  $\Delta p_{j,i}$  is the pressure difference (Pa), and  $\rho$  is the air density. The pressure difference,  $\Delta p_{j,i}$ , is calculated differently for vertical and horizontal interfaces [12].

Mixed sub-zones contain flow elements such as jets, plumes, and boundary layers. Thus, in a mixed sub-zone, both "flow-element" and "non-flow-element" parts exist. The flow between the non-flow-element parts are treated as standard sub-zones. The flow-element parts, on the other hand, are isolated volumes and are independent from the non-flow-element parts [12].

In this study, one type of flow-element, a circular thermal vertical jet, which describes the airflow from a ceiling diffuser, is used and is introduced here. The velocity distribution for this jet can be described in Figure 1. In Figure 1, the index  $m$  refers to the axis of the jet and the index  $o$  to the initial position of the jet (at the ceiling where  $z = 0 \text{ m}$  for this study). The area of the inlet is  $A_o$  ( $\text{m}^2$ ). The constant  $K_a$  represents the apparent length of the constant velocity zone measured from the inlet [14]. The initial temperature difference,  $\Delta T_o$ , is the temperature difference between the inlet and room temperature ( $^\circ\text{C}$ ). The velocity along the jet axis is  $w_m$ , and the initial jet velocity is  $w_o$ . Finally,  $z$  is the distance from the inlet measured along the jet axis (m). The plus sign inside the brackets is used when the momentum of the jet is in the same

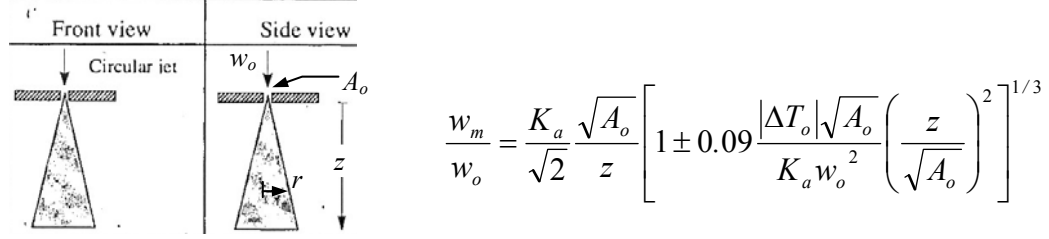


**Figure 1.** Diagram ([13]) and velocity equation for circular thermal vertical jet [12].

direction as gravity, as it is in this study. Conversely, when the forces are in opposite directions, the minus sign is used.

The radius of the jet increases as the distance from the supply outlet increases. The increase in jet radius,  $r$ , is assumed to be approximately linear and is expressed as [12]:

$$\frac{w}{w_m} = \exp \left[ -k \left( \frac{r}{z} \right)^2 \right] \quad (2)$$

Thus, the ratio of the mass flow rate for the jet is:

$$\frac{z_m(z)}{z_{mo}} = \frac{\pi}{\sqrt{2}} \frac{K_a}{k} \frac{z}{\sqrt{A_o}} \left[ 1 \pm 0.09 \frac{|\Delta T_o| \sqrt{A_o}}{K_a w_o^2} \left( \frac{z}{\sqrt{A_o}} \right)^2 \right]^{1/3} \quad (3)$$

where the mass flow rate at any distance  $z$  from the inlet is  $z_m(z)$  and the initial mass flow rate is  $z_{mo}$ . This relationship is used to estimate the mass flow rate between the flow-element portions of the mixed sub-zones.

### 2.3 Building Model

Two spaces are modeled for this study. One is a typical office and the other a large hall. The office is 5.5 m × 5.5 m × 2.6 m high. The large hall is 11 m × 10 m × 3.6 m high. Each space was first sub-divided into sub-zones. Sub-division of the office is shown in Figure 2. Sub-division of the large hall is not shown for brevity. The office was thus sub-divided into 80 sub-zones (5 × 4 × 4 cells) and the large hall into 486 sub-zones (9 × 9 × 6 cells). Selection of the size of the sub-zone should be carefully considered. For mixed sub-zones, the size of the sub-zone must be sufficiently large to capture the flow element [12]. Thus, Eq. (2) is used to determine the minimum width and depth (since the jet is circular) of all mixed sub-zones. In this study, it was found to be 1.4 m. For standard sub-zones, a general guideline of 0.25 to 1.5 m is recommended in the literature [7]. Thus, the average size of each sub-zone is 1.3 m<sup>2</sup> × 0.5 m high. Wurtz et al. [10] conducted a study on a two dimensional space using a zonal model. The grid systems used were 3 × 3 and 6 × 6. It was shown that increasing the number of grids did not result in more accurate airflow results when compared to CFD results.

Each simulated room is assumed to have no windows and no doors. It is also assumed that leakage to and from the ambient is negligible. The initial temperature of each room is 21°C, and the temperature of the inlet jet is 13°C. All inlet jets are modeled as delivering 400 cfm through a 0.7 m-diameter diffuser. The office has one supply diffuser and one exhaust. The large hall has four supply diffusers and four exhausts. Figure 2 shows the location of the supply and exhaust in the office. Locations of the supply diffusers and exhausts in the large hall are discussed along with releasing scenarios in Sec. 2.4. Though COwZ is able to perform a thermal

simulation, accounting for temperature variations within a sub-zone [12], this feature was not implemented for this study. For each room, two cases are considered: one using the multi-zone model approach and the other using the zonal model approach. Transient airflow simulation is chosen for both cases. Two exposures are assessed at opposite corners in the office. Four exposures are assessed in the large hall, equally distributed throughout the space. Their locations are marked in Figure 3. Both instantaneous exposure and cumulative exposure are assessed. Instantaneous exposure is defined as [1]:

$$E = \int_{t_1}^{t_2} C(t) dt \quad (4)$$

Cumulative exposure is then simply the summation of instantaneous exposure values over any given time period. The cumulative exposure is the "exposure" used as one of the design objectives. In this study, the time step was one minute. The total simulation period was two hours.

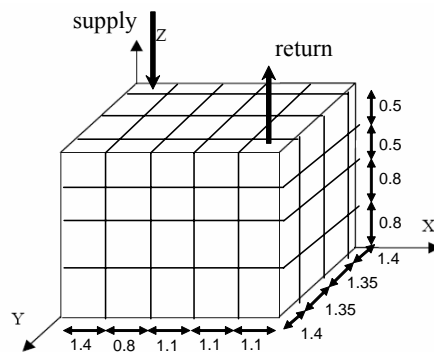


**Figure 2.** Subdivision of the office into sub-zones.

## 2.4 Contaminant Releasing Scenarios

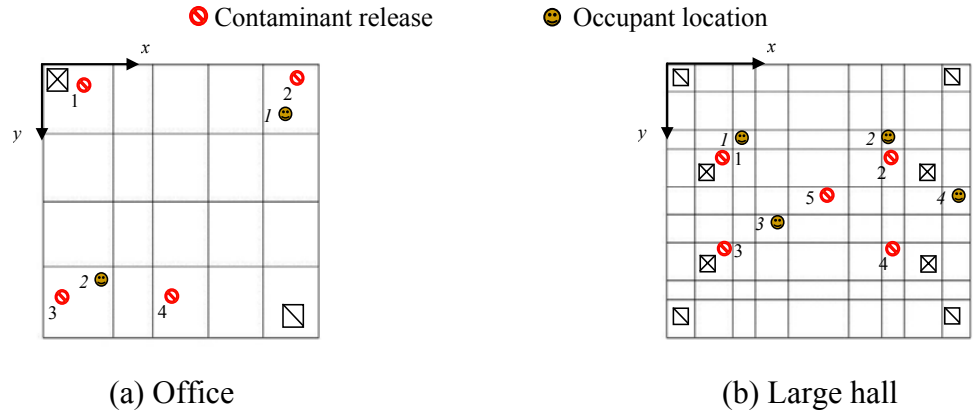
Sarin gas, a highly toxic nerve agent of high volatility, is selected as a typical CBW agent to be simulated in this study. The source is modeled as a constant source (5 mg/s) that is present at the start of the simulation and lasts for one minute. Four releasing scenarios are considered in the small office, and five releasing scenarios for the large hall. The number of releasing scenarios is chosen based on possible targets for effective dispersion or ease of accessibility. Sub-zone locations names are given by their respective  $x$ ,  $y$ , and  $z$  cell index. For instance, in Figure 3a, the first releasing location is 111. The second releasing location is 511, and so on. All contaminants are released on the floor. All occupants are located on the floor. For the office, release location 1 is under the supply diffuser. Release locations 2 and 3 are chosen near the occupants. Release location 4 is chosen along the wall where a door may be located. For the large hall, release locations 1, 2, 3, and 4 are under respective supply diffusers. Release location 5 is arbitrarily chosen in the center of the hall.

## 3. RESULTS AND DISCUSSION

### 3.1 Simulation Results

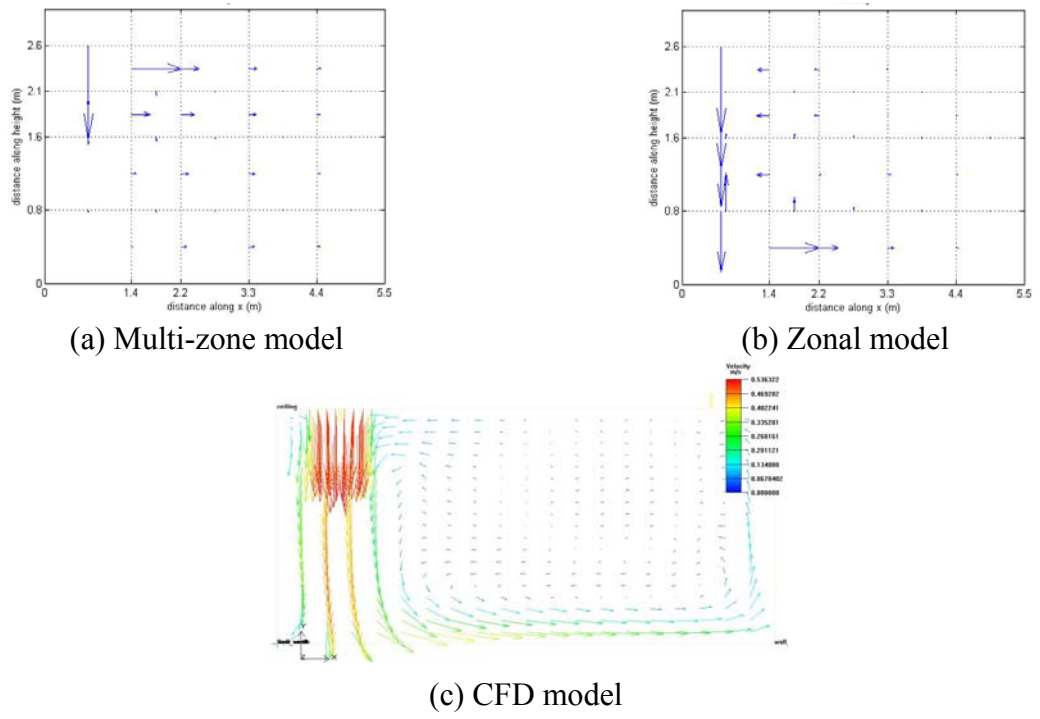
#### 3.1.1 Airflow Results

The airflow rate through each airflow path after the contaminant is released remains relatively steady during the simulation period. It is not affected when the contaminant releasing

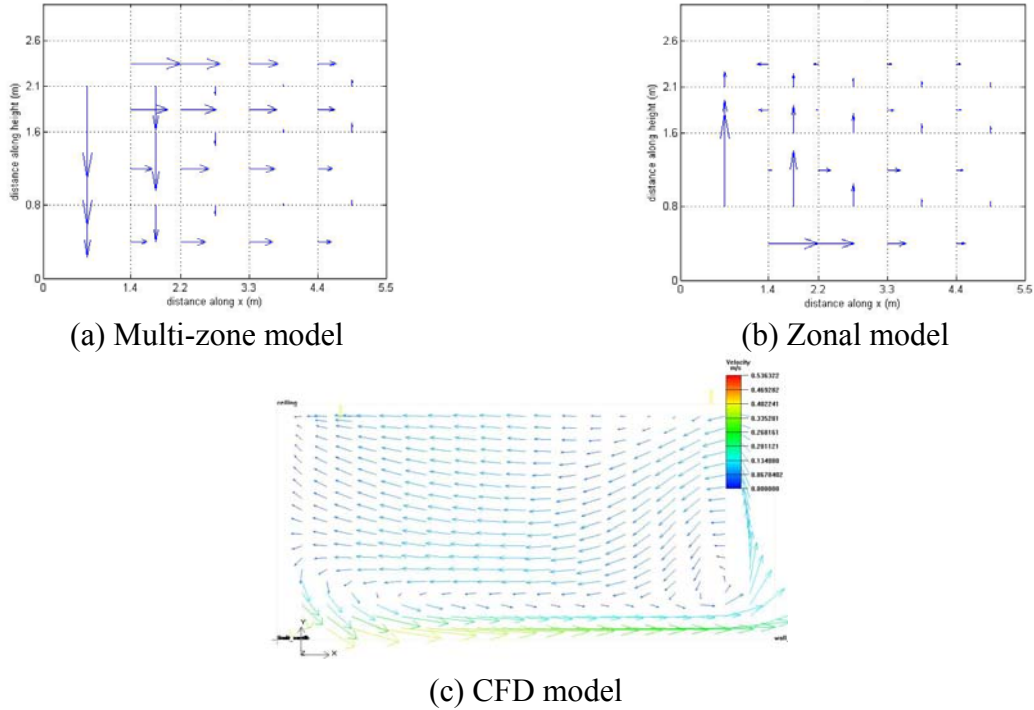


**Figure 3.** Release locations and occupants (Note: Figures are not drawn to scale)

location is changed. The figures below compare the airflow patterns from the multi-zone case, the zonal model case, and CFD results using AIRPAK [15] for the office. Figure 4 shows the airflow results through the diffuser, i.e. through  $y$ -cell-1. The striking difference between the multi-zone model and the zonal model is the representation of the inlet jet. The influence of the supply air is more pronounced in the zonal model and thus agrees more with the CFD result. The multi-zone model has more areas of stagnant air than the zonal model. Furthermore, the recirculation pattern predicted by the zonal model more resembles that predicted by the CFD model.



**Figure 4.** Comparing airflow patterns different models through the supply diffuser in the office.



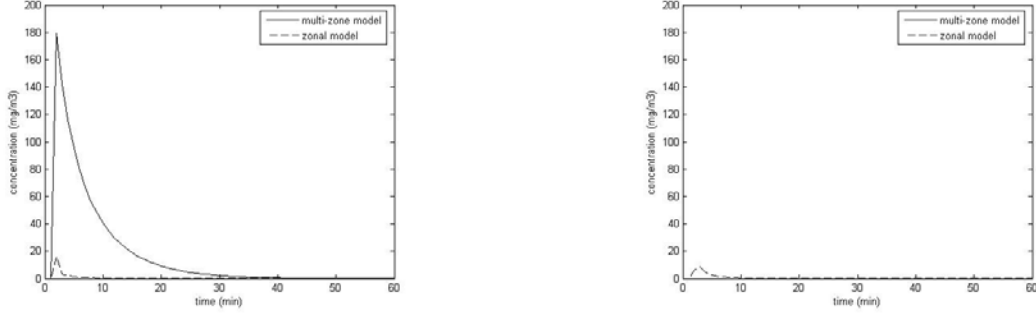
**Figure 5.** Comparing airflow patterns different models through the center of the office.

Figure 5 shows the airflow results through the center of the office ( $y = 2.75$  m). The multi-zone model shows the influence of the supply air pushing flow downward. The recirculation is generally clockwise. This does not agree with the CFD result. CFD predicts the bulk of the air above the floor moving to the left and a large amount of air near the floor moving to the right. This trend is more pronounced in the zonal model. Airflow results through the exhaust from the multi-zone model and zonal model are nearly identical and also agree well with the CFD result. Therefore, they are not shown for brevity.

Comparisons of the airflow simulation results from the multi-zone model and zonal model for the large hall case are similar to those reported for the office case and are thus not reported here.

### 3.1.2 Contaminant Results

Both the rate of the concentration variation and the peak value of the concentration vary from sub-zone to sub-zone. Figure 6 shows the contaminant concentration in sections of the office as a result of releasing scenario 1. The concentration profiles in the release sub-zone (Figure 6a) and in the center (half-way in the  $x$ -,  $y$ -, and  $z$ -directions) of the office (Figure 6b) are compared for each airflow model. Figure 6a shows that the concentration in the release sub-zone using the multi-zone model is much greater than that using the zonal model. This difference can be attributed to the fact that the multi-zone model did not predict a large amount of airflow exchange between the particular sub-zone and the surrounding sub-zones (Figure 4). The inclusion of a jet model in the zonal approach allows greater circulation of air and thus transport of contaminants throughout more areas of the room, which is probably a more realistic representation of actual conditions. Figure 6b shows that the concentration in the center of the room calculated by the multi-zone model is zero. This is attributed to two things. One, airflow



(a) Contaminant concentration in the release sub-zone for multi-zone and zonal model

(b) Contaminant concentration in the center of the office for both multi-zone and zonal model

**Figure 6.** Contaminant concentration in the office for the first releasing scenario.

through the release sub-zone is small, thus, the contaminant is not being distributed to the rest of the room. Two, airflow to the center of the room is also small. Furthermore, the concentration calculated by the zonal model in the center of the room is of similar magnitude to that in the release sub-zone. This indicates a more thorough distribution of the contaminant, which is more realistic.

Figure 7 shows the concentration profiles for the release sub-zone and the center of the large hall. The concentration profile for the center of the hall has been scaled for clarity. As exhibited in the office, the multi-zone model predicts much higher concentration in the release sub-zone compared to that predicted by the zonal model. Furthermore, the concentration in the center of the room calculated by the multi-zone model is zero, as was the case inside the office. The concentration calculated by the zonal model in the center of the room probably more closely resembles actual conditions.

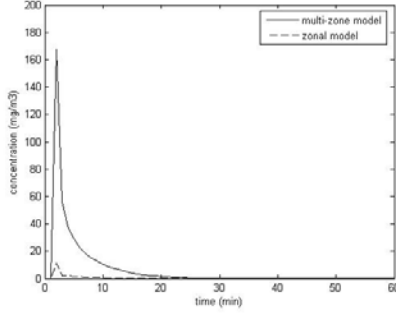
The multi-zone model predicts stronger ventilation dilution effects in the large hall compared to the office. This is observed by the slopes in Figure 6a and Figure 7a. Since the supply airflow rate for the diffusers modeled are identical, the change in slope is questionable. The ventilation dilution effects predicted by the zonal model are very similar in both the office and large hall.

### 3.2 Sensor System Design Results

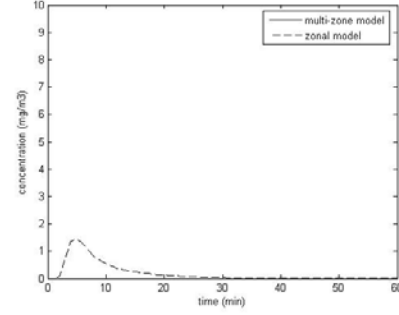
The air flow rates, contaminant concentration, and occupant exposure are simulated for four releasing scenarios in the office and five releasing scenarios in the large hall. A sensor system is designed using the Matlab GA optimization toolkit [16] after obtaining the simulation results. The selection of sensor quantities and location(s) for a fixed sensitivity are discussed in Sec. 3.2.1. Results from the office and large hall simulation are discussed separately in Secs. 3.2.1.1 and 3.2.1.2. The objective functions for the GA are detection time and total occupant exposure. The objective detection time,  $J_{det}$ , is defined as [3]:

$$J_{det} = \sum_{k=1}^N p_k \times t_{det-k} \quad (5)$$

where  $p_k$  is the probability for the  $k$ th releasing scenario to occur and  $N$  is the number of releasing scenarios.



(a) Contaminant concentration in the release sub-zone inside the large hall for both multi-zone and zonal model



(b) Contaminant concentration in the center of the large hall for both multi-zone and zonal model

**Figure 7.** Contaminant concentration in the large hall for the first releasing scenario.

Total occupant exposure,  $E_k$ , for the  $k$ th releasing scenario is defined as [3]:

$$E_k = \sum_{m=1}^S \sum_{t=0}^{t_{\text{det}}-k} \text{Exp}(m, t) \quad (6)$$

where  $\text{Exp}(m, t)$  is the occupant exposure for the  $m$ th occupant at time  $t$  and  $S$  is the number of occupants. Thus, for all  $N$  releasing scenarios, the objective function based on total occupant exposure,  $J_{\text{exp}}$ , is defined as [3]:

$$J_{\text{exp}} = \sum_{k=1}^N p_k \times E_k \quad (7)$$

### 3.2.1 Fixed sensitivity

The sensor sensitivity is a fixed value, such as  $0.03 \text{ mg/m}^3$  (portable sensor, \$7500 each [17]). The authors will discuss sensor system design results for the office and the large hall separately. Within each section is also a discussion on resulting sensor system designs using the multi-zone and zonal model, respectively. Analysis on the effects of changing the sensor sensitivity on the sensor system design is presented in [3].

#### 3.2.1.1 Results from office

As discussed in a previous study conducted by the authors [3], when the sensor quantity is equal to the number of releasing scenarios, numerous configurations of sensors exist. Therefore, this study focuses on sensor quantities less than the number of releasing scenarios for acceptable detection times and exposure levels.

The objective of this study is to compare sensor system designs resulting from the use of multi-zone and zonal models. Future studies will include comparisons with CFD simulations. Table 1 summarizes sensor locations for one- and two-sensor configurations using both minimum detection time and minimum occupant exposure as objective functions for GA. The optimal location for sensors was first determined using the multi-zone model. The detection time and occupant exposure for the same sensor system (quantity and locations) were then determined for the zonal model. In general, sensor system design using the zonal model reduces detection time and total occupant exposure. Table 1 shows that the minimum detection time for

**Table 1.** Sensor design in office for sensor with 0.03 mg/m<sup>3</sup> sensitivity.

Configuration Number	Quantity	Objective	Locations	Fitness value	
				Multi-zone	Zonal
1	2	D	221, 542	1 min	1 min
2	2	D	311, 542	1 min	1 min
3	2	E	321, 542	1.317E-4 kg/kg	1.251E-4 kg/kg
4	2	<i>E</i>	<i>141, 533</i>	<i>1.317E-4 kg/kg</i>	<i>1.251E-4 kg/kg</i>
5	1	D	542	1.5 min	1.25 min
6	1	D	441	1.5 min	1.25 min
7	<i>1</i>	<i>E</i>	<i>542</i>	<i>1.351E-4 kg/kg</i>	<i>1.302E-4 kg/kg</i>
8	1	E	441	1.666E-4 kg/kg	1.616E-4 kg/kg

Note: "D" is detection time; "E" is occupant exposure. Italics symbolizes selected configuration.

two sensors is one minute using "D" as the objective function. Since this detection time is also guaranteed when using "E" as the objective function, configurations numbers 1 and 2 need no consideration. Thus, two remaining configuration alternatives exist. However, for practical purposes, sub-zone 542 and 533 can be considered the same because they are no more than one sub-zone apart. One possible location for other sensor is near Occupant 2 (Figure 8). This location is a logical choice because Occupant 2 is near the exhaust. The bulk of the recirculated air will travel to the exhaust and by Occupant 2.

Two possible locations are selected for a sensor quantity of one. For reasons already discussed, configurations 5 and 6 need no consideration. Since a sensor placed in sub-zone 542 results in less total exposure no matter the airflow model used, it is the desired location (Figure 8). Nevertheless, sub-zone 441 and 542 can be considered the same because they are only one sub-zone apart from each other. Figure 8 graphically summarizes the sensor system design for two sensors and one sensor in the office.

### 3.2.1.2 Results from large hall

Procedures for determining and comparing candidate sensor configurations are similar to those used for the office. Table 2 summarizes possible sensor locations for one- and three-sensor configurations. When the sensor quantity is three and objective function is "D", the detection time is one minute using the zonal model and 1.6 minutes using the multi-zone model. In practice, a detection time of less than two minutes is acceptable. When the objective function is "E", the zonal model minimizes the total occupant exposure to a greater extent than the multi-zone model. Since using "E" as the objective function also guarantees a detection time of two minutes, configuration 3 is selected as the optimal sensor system configuration for three sensors. For this configuration, the zonal model is able to minimize the total occupant exposure by about 80% compared to that calculated by the multi-zone model.

When the sensor quantity is one and the objective function is "D", the detection time calculated using the multi-zone model is over five minutes. It is unacceptable for this particular study. It is interesting at this point to note that the detection time using the zonal model is one minute no matter the sensor quantity. Because the two-minute detection limit holds true when "E" is selected as the objective function, configuration 5 is selected as the optimal sensor location as it results in the lowest total occupant exposure for both airflow models. As was the case for a

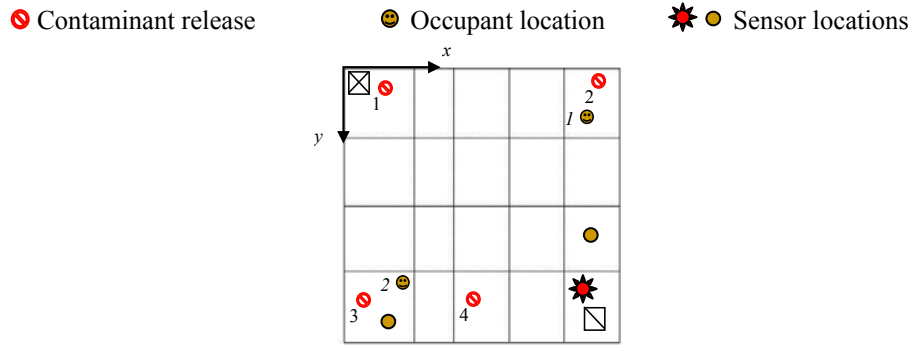


**Figure 8.** Sensor system design locations for the office.

sensor quantity of three, using the zonal model results in about a 75% reduction in total occupant exposure.

Figure 9 graphically summarizes the sensor system design for three sensors and one sensor in the large hall. When the sensor quantity is three, one sensor is located near the first release location and the other two are dispersed among the other occupants. When the sensor quantity is one, it is placed near the first release location.

**Table 2.** Sensor design in large hall for sensor with  $0.03 \text{ mg/m}^3$  sensitivity.

Configuration Number	Quantity	Objective	Locations	Fitness value	
				Multi-zone	Zonal
1	3	D	241, 541, 561	1.6 min	1 min
2	3	E	531, 626, 635	9.096E-5 kg/kg	9.962E-6 kg/kg
3	3	<i>E</i>	<i>441, 734, 872</i>	<i>8.329E-5 kg/kg</i>	<i>1.371E-5 kg/kg</i>
4	1	D	241	5.2 min	1 min
5	1	<i>E</i>	<i>441</i>	<i>8.329E-5 kg/kg</i>	<i>1.662E-5 kg/kg</i>
6	1	E	426	8.515E-5 kg/kg	2.225E-5 kg/kg

Note: "D" is detection time; "E" is occupant exposure. Italics symbolizes selected configuration.

#### 4. CONCLUSION

Indoor contaminant sensor system design to protect a building from CBW attack is discussed in this study. Contaminant concentration and occupant exposure are simulated using both a multi-zone and zonal airflow model for two spaces: an office and a large hall. Four releasing scenarios are simulated in the office, and five releasing scenarios in the large hall. GA is used to optimize the sensor system using either minimum detection time or minimum occupant exposure as the objective function.

First, comparisons of predicted airflows were made between the multi-zone and zonal model. In the case of the office, CFD results were also compared. Generally, the zonal model made more accurate predictions on overall flow patterns, i.e. capturing supply inlet jets and regions of recirculation well. The supply inlet jet seems to have little or no influence on surrounding air when the multi-zone model is used. Second, comparisons were made on calculated concentrations in various sub-zones of interest. Concentration profiles were obtained

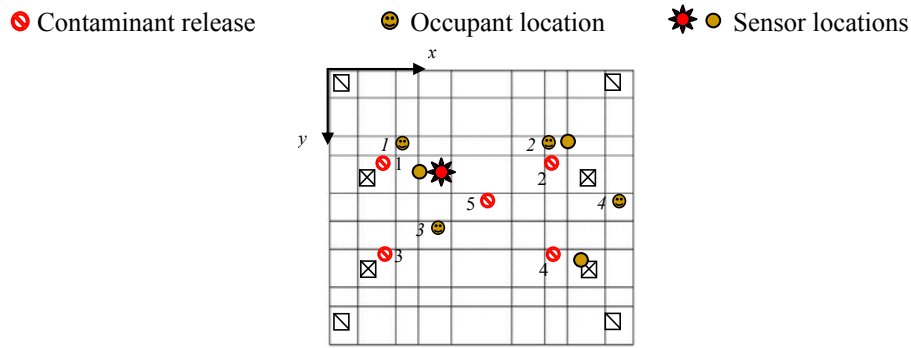


**Figure 9.** Sensor system design locations for the large hall.

for both rooms using both models for the release sub-zone and in the center of the room. Areas of stagnation predicted by the multi-zone model exhibited both unrealistically high and unrealistically low concentrations. Furthermore, the magnitude of the maximum concentration predicted by the multi-zone model is much larger than that of the calculated occupant exposure. On the other hand, the magnitude of the maximum concentration and the occupant exposures using the zonal model are much more similar. Lastly, GA optimization was employed for both models to determine optimal sensor system design configurations. In general, both the detection time and total occupant exposure obtained using the zonal model are lower than those obtained using the multi-zone model. Nevertheless, the set detection limit of two minutes was never exceeded. Therefore, optimal sensor locations were selected on the basis of minimizing total occupant exposure. In the case of the office, what seemed like different sensor configurations were actually the same from a practical viewpoint. This is because the sensor locations found were only one sub-zone apart. In the case of the large hall, different sensor configurations were actually different. This is due to the increased size of the large hall.

For small rooms such as an office, using either the multi-zone model or zonal model does not greatly affect the sensor system design. On the other hand, for larger rooms such as a large hall, the effect of the airflow model on the sensor system design is not as straightforward. The selection would be determined by the minimum detection time and allowable exposure limit ascribed to any individual application.

## 5. FUTURE WORK

The selection of optimal sensor configurations for this study was based on the airflow and contaminant dispersion results from both a multi-zone and zonal model. Future work will compare sensor system designs using airflow and contaminant dispersion from CFD models to the present study.

## 6. ACKNOWLEDGEMENTS

The authors would like to thank the National Science Foundation (NSF), through grant NSF CMS SGER 0549959, for support of this study. Partial support was provided by NSF through the Graduate Research Fellowship Program. The authors would also like to extend appreciation to Dr. Zhengen Ren of the QUESTOR Centre and School of Electrics, Electrical and Computer Science of the The Queen's University Belfast for his work and technical support on COwZ. Thanks also to Dr. David Lorenzetti of the Lawrence Berkeley National Laboratory for his work and support on COMIS.

## REFERENCES

1. Walton, G.N. and W.S. Dols, 2005, CONTAM 2.4 User Guide and Program Documentation, National Institute of Standards and Technology, NISTIR 7251, Gaithersburg, MD.
2. Mora, L., Gadgil, A. J., Wurtz, E., 2003. "Comparing zonal and CFD model predictions of isothermal indoor airflows to experimental data," *Indoor Air*, 13(2). 77-85.
3. Chen, Y.L. and J. Wen, 2007. "Sensor System Design for Building Indoor Air Protection," *Building and Environment*, Accepted.
4. Arvelo, J., A. Brandt, R. P. Roger, and A. Saksena, 2002. "An Enhanced Multizone Model and Its Application to Optimum Placement of CBW Sensors," *ASHRAE Transactions*, 108(2). 818-825.
5. Zhai, Z., J. Srebric, Q. Chen, 2003. "Application of CFD to Predict and Control Chemical and Biological Agent Dispersion in Buildings," *International Journal of Ventilation*, 2(3). 251-264.
6. Feustal, H.E. and B.V. Smith, 1997, COMIS 3.0 - User's Guide, Lawrence Berkeley National Laboratory,
7. Ren, Z. and J. Stewart, 2003, COwZ User's Guide: Zonal indoor source emission and dispersion model, Version 1, The School of Computer Science and QUESTOR Centre,
8. Musy, M., E. Wurtz, F. Winkelmann, and F. Allard, 2001. "Generation of a zonal model to simulate natural convection in a room with a radiative/convective heater," *Building and Environment*, 36(5). 589-596.
9. Inard, C., H. Bouia, and P. Dalicieux, 1996. "Prediction of air temperature distribution in buildings with a zonal model," *Energy and Buildings*, 24(2). 125.
10. Wurtz, E., J.-M. Nataf, and F. Winkelmann, 1999. "Two- and three-dimensional natural and mixed convection simulation using modular zonal models in buildings," *International Journal of Heat and Mass Transfer*, 42(5). 923.
11. Haghghat, F., Y. Li, and A.C. Megri, 2001. "Development and validation of a zonal model - POMA," *Building and Environment*, 36(9). 1039.
12. Ren, Z., *Enhanced modelling of indoor air flows, temperatures, pollutant emission and dispersion by nesting sub-zones within a multizone model*. 2002, The Queen's University of Belfast.
13. Heiselberg, P., S. Murakami, and R. C-A, 1998, Ventilation of large spaces in buildings: analysis and prediction techniques, Aalborg University, IEA Annex 26: Energy efficient ventilation of large enclosures, Denmark.
14. Koestel, A., 1954. "Computing Temperatures and Velocities in Vertical Jets of Hot or Cold Air," *Heating, Piping & Air Conditioning*, (June). 110-148.
15. FLUENT, 2002, Airpak 2.1 User's Guide, Fluent Inc., Lebanon, NH
16. Mathworks, 2004, Genetic Algorithm and Direct Search Toolbox, The Mathworks Inc., Natick, MA.
17. Institute of Medicine and Medical Research Council, 1999, Chemical and Biological Terrorism - Research and Development to Improve Civilian Medical Response, Institute of Medicine and Medical Research Council, National Academies Press, Washington D.C.,